Analytical Biochemistry 437 (2013) 1–9

Contents lists available at SciVerse ScienceDirect

Analytical Biochemistry

journal homepage: www.elsevier.com/locate/yabio

Construction of an amperometric D-amino acid biosensor based on D-amino acid oxidase/carboxylated mutliwalled carbon nanotube/copper nanoparticles/polyalinine modified gold electrode

Suman Lata, Bhawna Batra, Pankaj Kumar, C.S. Pundir *

Department of Biochemistry, M.D. (Maharshi Dayanand) University, Rohtak 124 001, India

ARTICLE INFO

Article history:
Received 15 December 2012
Received in revised form 23 January 2013
Accepted 24 January 2013
Available online 8 February 2013

Keywords:
Amino acid
Biosensor
Carbon nanotubes
Copper nanoparticles
Enzymes

ABSTRACT

An improved D-amino acid biosensor was constructed based on covalent immobilization of D-amino acid oxidase onto carboxylated mutliwalled carbon nanotube/copper nanoparticles/polyalinine hybrid film electrodeposited on gold electrode. The biosensor exhibited an optimal response within 2 s at pH 8.0 and 30 °C when polarized at 0.09 V. There was a linear relationship between biosensor response (μA) and D-alanine concentration ranging from 0.001 to 0.7 mM. The sensitivity of the biosensor was 54.85 μA cm^{-2} mM^{-1} with a lower limit of detection of 0.2 μM (signal/noise = 3). The enzyme electrode was used 150 times over a period of 4 months. The biosensor measured the D-amino acid level in fruit juices.

The level of amino acids in foods is used as a measure of their nutritive value. Food materials contain large quantities of non-natural substances of external origin that influence their digestibility to a considerable degree [1]. Foodstuffs are the most significant sources of non-natural D-amino acids (DAAs).[1] Racemization of the naturally occurring L-form of amino acid into its D-form can decrease the nutritional value of food products [2]. Modern food industry technology applies a diverse range of procedures to modify the characteristics of proteins to improve the flavor, consistency, and non-perishability of food [3]. Heat and/or alkali treatment have been used preferentially to manufacture the products possessing particular characteristics, form, and function as they give rise to the DAA level [4]. DAAs are found in commercial foodstuffs and alcoholic beverages, which are generated during technological processing. The DAA level in fruit juices elevates in association with microbial growth in samples [5] because D-isomers of amino acids are common constituents of the bacterial cell wall [6]. The presence of DAAs in proteins leads to a decrease in digestibility and the availability of L-amino acids (LAAs). Changes in DAA level in the brain are associated with several neurological and psychiatric diseases and, thus, have a major impact on the organism as a whole. Therefore, the determination of DAAs in foodstuffs is very important.

Various analytical techniques have been employed for determination of DAAs, including high-performance liquid chromatography (HPLC), gas chromatography [7–9], capillary electrophoresis [7], spectrophotometry [10], and chiral HPLC based on two-dimensional HPLC separations [11]. All of these methods are very sensitive, reliable, and reproducible, but they are very expensive and require time-consuming sample preparation, unportable and specialized equipment, and trained persons to operate. Biosensors overcome these problems, because they are comparatively more simple, fast, responsive, and sensitive and are highly specific, accurate, and portable after miniaturization; thus, they are suitable for clinical, nutritional, biomedical, and pharmaceutical analysis [12].

A number of DAA biosensors have been reported based on immobilization of D-amino acid oxidase (DAAO) onto Prussian Blue (PB) film electrodeposited onto gold (Au) electrode [13] graphite working electrode [14] gel matrix of hydroxyethyl cellulose [15], polyethylenimine modified electrode [10], thin layer Plexi cell [16], rhodonized carbon electrode [12], amine modified silica gel [17], Teflon electrode matrix [18], Teflon membrane [19], eggshell membrane [20], PB and single-walled carbon nanotubes (SWCNTs) [21], Amberzyme oxirane support [22], poly(*o*-phenylenediamine) and Nafion modified platinum–iridium disk electrode [23], and

* Corresponding author. Fax: +91 126274640.
E-mail address: pundircs@rediffmail.com (C.S. Pundir).

[1] *Abbreviations used:* DAA, D-amino acid; HPLC, high-performance liquid chromatography; DAAO, D-amino acid oxidase; PB, Prussian Blue; Au, gold; SWCNT, single-walled carbon nanotube; CuNP, copper nanoparticle; CNT, carbon nanotube; PANI, polyaniline; C-MWCNT, carboxylated multiwalled carbon nanotube; D-Ala, D-alanine; EDC, *N*-ethyl-*N*′-(3-dimethylaminopropyl)carbodiimide; NHS, *N*-hydroxysuccinimide; DW, double distilled water; UV, ultraviolet; TEM, transmission electron microscope; XRD, X-ray difractometer; SEM, scanning electron microscopy; CV, cyclic voltammetry; FTIR, Fourier transform infrared; CV, coefficient of variation.

0003-2697/$ - see front matter © 2013 Elsevier Inc. All rights reserved.
http://dx.doi.org/10.1016/j.ab.2013.01.030

nickel hexacyanoferrate/polypyrrole/glassy carbon electrode [24]. In these biosensors, the immobilized DAAO electrode brings about the stereospecific oxidative deamination of DAAs as follows:

$$\text{D-Amino acid} + O_2 + H_2O \overset{\text{DAAO}}{\rightarrow} \alpha - \text{keto acid} + NH_3 + H_2O_2 \quad (1)$$

The H_2O_2 generated is measured electrochemically, which is directly proportional to the concentration of DAAs. However, these biosensors suffer from low stability, reusability, and sensitivity; thus, they still need to be improved.

The use of nanomaterials in construction of enzyme electrodes has led to improvement in their stability, reusability, sensitivity, and anti-interference ability. Among the various metal nanoparticles, copper nanoparticles (CuNPs) have attracted much attention because of their catalytic and optical properties and high electrical and heat conductivity [25].

Carbon nanotubes (CNTs) have also been employed to improve the analytical performance of biosensors because of their distinctive physical and chemical properties, which promote fast electron transfer. Composite materials based on integration of CNTs with some other nanomaterials possess properties of the individual components with a synergistic effect. Due to its facile preparation, high conductivity, and good environmental stability, a conducting polymer has become the most attractive one for construction of CNT-based composites [26]. Polyaniline (PANI) is one of the most intensively investigated conducting polymers due to its excellent stability in different solutions, good electronic properties, and strong biomolecular interactions [27]. Thus, PANI/CNT composites synthesized chemically or electrochemically have attracted interest to improve the electrical conductivity, electrochemical capacitance, and electrocatalytic properties of enzyme electrodes [28].

Here we describe the construction of an improved amperometric DAA biosensor by covalently immobilizing DAAO onto carboxylated multiwalled carbon nanotube (c-MWCNT)/CuNPs/PANI/Au electrode, its evaluation, and its application in measurement of DAAs in fruit juices.

Materials and methods

Materials used

Sephadex G-100, DAAO from porcine kidney (EC 1.4.3.6, 0.05 U/mg solid), and DEAE–Sephacel from Sigma–Aldrich (USA), D-alanine (D-Ala), ferrous chloride, *N*-ethyl-*N*′-(3-dimethylaminopropyl) carbodiimide (EDC), *N*-hydroxysuccinimide (NHS), and ferric chloride from SRL (Mumbai, India), and c-MWCNTs from Intelligent Materials (Panchkula, India) were used. All other chemicals used were of analytical reagent (AR) grade. Gold wire and fruit juices of different brands were purchased from the local market. Double distilled water (DW) was used in all experimental studies.

Assay of free DAAO

The assay of free DAAO was carried out as described in Ref. [29] with modification. It was based on quantification of H_2O_2, generated from oxidation of D-Ala catalyzed by DAAO, using a color reaction consisting of 4-aminophenazone, phenol, and peroxidase as a chromogenic system. The reaction mixture consisting of 0.7 ml of Tris–HCl buffer (pH 8.0, 0.05 M), 0.1 ml of D-Ala solution (0.1 mM), and 0.1 ml of DAAO solution (0.5 U/ml) was incubated at 37 °C for 10 min. Then 1 ml of color reagent (50 mg of 4-aminophenazone, 100 mg of phenol, and 1.0 mg of horseradish peroxidase in 100 ml of 0.4 M sodium phosphate buffer [pH 7.0] and stored in the dark at 4 °C) was added and incubated in the dark at 37 °C for 15 min to develop the color. A_{520} was read and H_2O_2 concentration was interpolated from its standard curve (A_{520} vs. concentration of H_2O_2). One unit of DAAO is defined as the amount of enzyme required to catalyze the formation of 1.0 μmol of H_2O_2 from oxidation of DAA per minute/milliliter under standard assay conditions.

Construction of DAAO/c-MWCNT/CuNPs/PANI modified Au electrode

Preparation of CuNPs

After 50 ml of aqueous solution of $NaBH_4$ (0.3 M) was added to 100 ml of aqueous solution of $CuSO_4$ (0.4 M), the solution was heated to 45 °C under continuous stirring. After 30 min, the solution was spilled out and filtered. The filtrate was washed three times with absolute ethanol and acetone separately and finally dried in a drying oven [30].

Characterization of CuNPs

The morphological characterization of CuNPs was carried out in an ultraviolet (UV) spectrophotometer (model 1700 A, Shimadzu), a transmission electron microscope (TEM, JEOL 2100 F) at Jawahar Lal Nehru University (New Delhi, India), and an X-ray difractometer (XRD, 122 Rigaku, D/Max2550, Japan) at Guru Jambheshwar University (Hisar, India) on a commercial basis.

Electrodeposition of c-MWCNT/CuNPs/PANI onto Au electrode

The surface of an Au wire (2 cm × 1 mm) was polished manually by alumina slurry (diameter = 0.05 μm) with a polishing cloth, washed thoroughly with DW, and then placed into ethanol, sonicated to remove adsorbed particles, and finally washed with DW three or four times. c-MWCNTs (1.0 mg) were suspended into a 4-ml mixture of concentrated H_2SO_4 and HNO_3 in a 3:1 ratio and then ultrasonicated for 3 to 4 h to get its finely dispersed black-colored solution. The dispersed c-MWCNT solution (0.1 ml) was mixed into a mixture of 0.5 ml of 0.2 M EDC and 0.5 ml of 0.2 M NHS (pH adjusted to 6.0) and kept at room temperature for 1 h. Aniline (200 μl) was added to 25 ml of 1 M KCl (as electrolyte) and electropolymerized onto the surface of cleaned Au electrode by cyclic voltammetry, that is, by applying 20 successive polymerization cycles from −0.15 to 0.30 V at a scan rate of 20 mV s^{-1} in a potentiostat–galvanostat (model AUT83785, Autolab, manufactured by Eco Chemie, The Netherlands). CuNP suspension (200 μl) and 1.0 ml of EDC/NHS activated c-MWCNT suspension were added to this 25 ml of 1 M KCl and electrodeposited onto PANI modified Au electrode by applying 20 polymerization cycles from −0.15 to 0.30 V at a scan rate of 20 mV s^{-1}. The resulting c-MWCNT/CuNPs/PANI modified Au electrode was washed thoroughly with DW to remove unbound matter and kept in a dry Petri plate at 4 °C.

Immobilization of DAAO onto c-MWCNT/CuNPs modified Au electrode

c-MWCNT/CuNPs/PANI/Au electrode was dipped into 1.5 ml of DAAO solution (0.5 U/ml) and kept overnight at 4 °C for immobilization. The modified electrode with immobilized DAAO was washed three or four times with 0.1 M Tris–HCl buffer (pH 8.0) to remove residual unbound protein. The resulting DAAO/c-MWCNT/CuNPs/PANI/Au electrode (i.e., enzyme electrode) was used as working electrode and stored at 4 °C when not in use.

Scanning electron microscopy

The working electrode was characterized by scanning electron microscopy (SEM) at different stages of its construction. The SEM images of bare Au electrode, c-MWCNT/CuNPs/PANI/Au, and DAAO/c-MWCNT/CuNPs/PANI/Au electrode were taken in a scanning electron microscope (Zeiss EV040) at Jawahar Lal Nehru University, New Delhi.

Cyclic voltammetry and testing of DAA biosensor

Cyclic voltammetry (CV) of c-MWCNT/CuNPs/PANI/Au electrode with and without DAAO was recorded in a potentiostat–galvanostat from −0.15 to 0.3 V versus Ag/AgCl as reference and Pt wire as counter electrode in 25 ml of 0.05 M Tris–HCl buffer (pH 8.0) containing 100 μl of 0.1 mM D-Ala.

Optimization of DAA biosensor

To optimize working conditions of the biosensor, effects of pH, incubation temperature, time, and substrate (D-Ala) concentration on biosensor response were studied. To determine the optimal pH, the pH was varied between 5.0 and 10.0 at an interval of 0.5 pH unit using the following buffers, each at a final concentration of 0.05 M: pHs 5.0 to 5.5 sodium succinate buffer, pHs 6.0 to 7.5 sodium phosphate buffer, and pHs 8.0 to 10.0 Tris–HCl buffer. Similarly to determine the optimal temperature, the reaction mixture was incubated at different temperature (15–50 °C) at an interval of 5 °C. The effect of D-Ala concentration on biosensor response was determined by varying the concentration of D-Ala in the range 0.001 to 1.0 mM. The current response (in μA) was recorded by applying different potentials ranging from −0.15 to −0.3 V.

Application of DAA biosensor in fruit juices

DAA content of fruit juices was determined by the current biosensor in the a similar manner as described above for its response measurement under its optimal working conditions except that D-Ala was replaced by fruit juice sample. The DAA content in fruit juices was interpolated from the calibration curve between D-Ala concentration and current (in μA) prepared under optimal assay conditions of enzyme electrode (Fig. 1).

Storage stability of DAAO/c-MWCNT/CuNPs/PANI/Au electrode

The storage stability of the enzyme electrode was studied for 4 months by measuring its response weekly. The electrode was stored dry at 4 °C, when not in use.

Results and discussion

Characterization of CuNPs

UV and visible spectra exhibited a strong absorbance peak at 600 nm, confirming the synthesis of CuNPs (Fig. 2A). A typical TEM image of CuNPs showed the spherical shape of CuNPs with an average size of 30 nm (Fig. 2B). The XRD patterns of CuNPs showed the characteristic peak of CuNPs (Fig. 2C). The XRD peaks of CuNPs corresponded well to the reflection of Cu (CCID file no. 040836, cubic). Two main characteristic peaks for Cu at $2\theta = 43.3°$ and 50.4°, corresponding to Miller indexes 111 and 200, were observed. The peak positions were in good agreement with literature values of face-centered cubic (fcc) Cu [31]. These observations confirmed that the resultant particles were pure CuNPs.

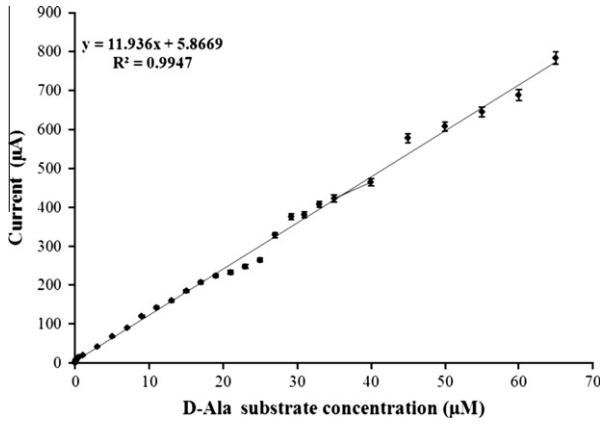

Fig.1. Effect of D-Ala concentration on response of DAA biosensor based on DAAO/c-MWCNT/CuNPs/PANI/Au electrode.

SEM studies of enzyme electrode

The SEM images of the surface of bare Au electrode, PANI/Au, c-MWCNT/CuNPs/PANI/Au electrode, and DAAO/c-MWCNT/CuNPs/PANI/Au electrode are shown in Fig. 3A–D, respectively. The SEM image of bare Au electrode showed a smooth and featureless morphology (Fig. 3A). Fig. 3B shows an SEM image of the fibrillar structure of PANI. Fig. 3C shows an SEM micrograph of c-MWCNT/PANI/CuNPs/Au electrode that exhibited its uniform, homogeneous, and cable-like morphology of the nano composite film, indicating that c-MWCNTs and CuNPs were well dispersed over the PANI layer in the hybrid film. After immobilization of enzyme on c-MWCNT/CuNPs/PANI hybrid film, the enzyme electrode showed the sporadic appearance of globular/beaded structure on the hybrid film (Fig. 3D), indicating that enzyme was successfully immobilized on the surface of c-MWCNT/CuNPs/PANI composite film.

Construction of D-amino acid biosensor

Fig. 4 provides the schematic representation of construction of enzyme electrode based on covalent immobilization of DAAO onto c-MWCNTs decorated with CuNPs and electrodeposited on the surface of Au electrode along with PANI. During construction of enzyme electrode, DAAO was immobilized covalently onto c-MWCNT/CuNPs/PANI/Au electrode through EDC/NHS activated c-MWCNTs. The reaction includes the formation of an intermediate ester (the product of condensation of the free –COOH groups of c-MWCNT/CuNPs/PANI composite film and NHS). The active ester intermediate reacts with the $-NH_2$ groups on the surface of enzyme to yield the final amide bond, confirming the covalent immobilization of enzyme on the surface of c-MWCNT/CuNPs/PANI composite film. The cyclic voltammograms of c-MWCNT/CuNPs/PANI/Au exhibited an enhanced current response, revealing that c-MWCNT/CuNPs/PANI/Au composite film has a large effective surface area and could provide composite matrix for faster kinetics. Hence, the c-MWCNT/CuNPs/PANI acting as electron transfer mediator helps in enhancing the biosensor response and, thus, increases its sensitivity. This covalent coupling of the enzyme onto c-MWCNT/CuNPs/PANI composite film does not allow the leaching of the enzyme during repeated washing of the enzyme electrode for its reuse. Earlier DAA biosensors suffered due to the leakage of enzyme on account of noncovalent coupling of enzyme onto the electrode [19,20,24].

Response measurements of DAA biosensor

The maximum response (current in μA) was observed at 0.09 V, which is lower/better than earlier DAA biosensors based on thin layer Plexi cell (0.45 V) [16] and nickel hexacyanoferrate/polypyrrole/glassy carbon electrode (0.25 V) [24]; hence, subsequent studies were carried out at this voltage. The low working potential is advantageous because it does not allow ionization of interfering compounds. Amperometric response of DAAO/c-MWCNT/CuNPs/PANI/Au was increased on the addition of 100 μl (0.1 mM) of D-Ala at the applied potential (0.09 V). When D-Ala was added into the buffer solution, the oxidation current rose steeply to reach a stable value (Fig. 5). The sensor responded very rapidly, producing 95% of the steady-state current within 2 s, which is less time than that needed for earlier biosensors based on eggshell membrane

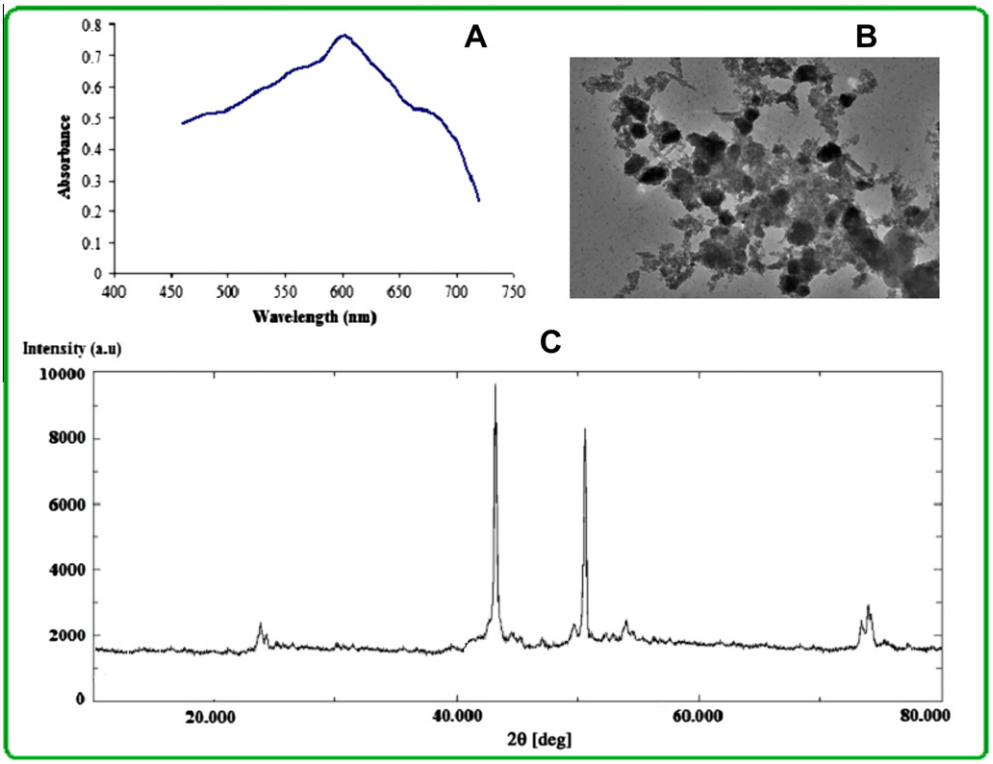

Fig.2. (A) UV–visible spectra of CuNPs. (B) TEM image of CuNPs. (C) XRD pattern of CuNPs.

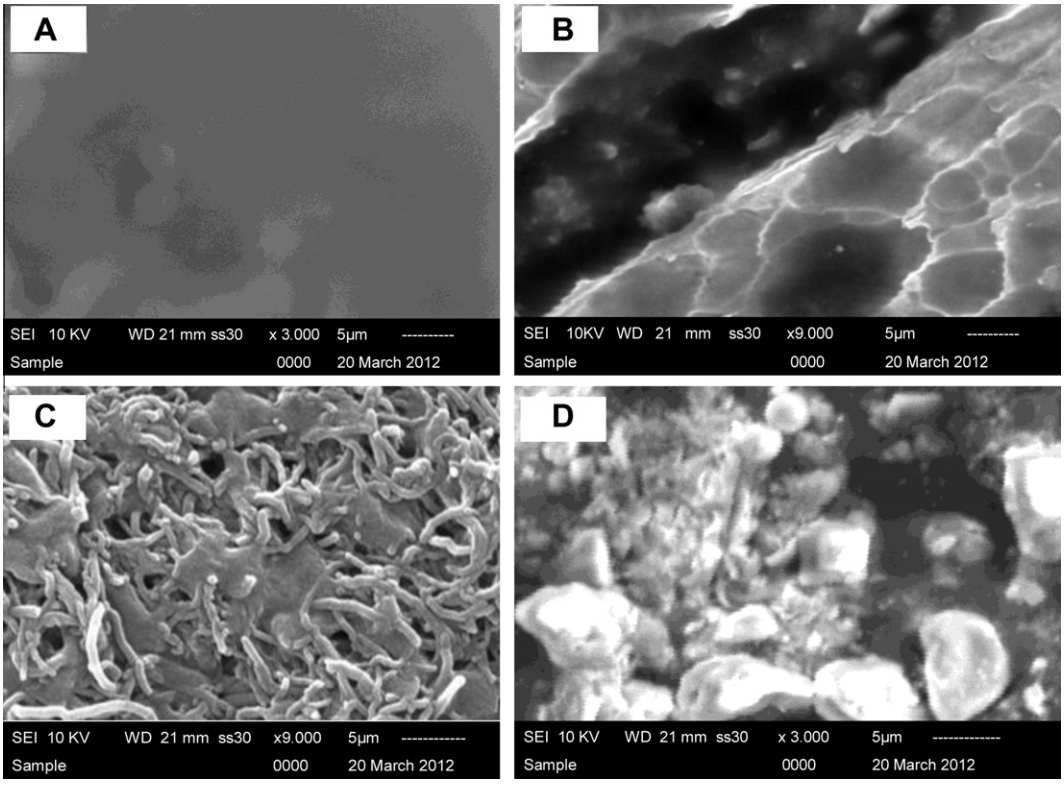

Fig.3. SEM images of bare Au electrode (A), PANI/Au electrode (B), c-MWCNT/CuNPs/PANI/Au electrode (C), and DAAO/c-MWCNT/CuNPs/PANI/Au electrode (D).

(1 min) [20] and Teflon membrane (10–15 min) [22]. This faster response can be attributed to the synergetic influence of c-MWCNT, PANI, and CuNPs composite film, which provides an environment for the enhanced electrocatalytic effect and a fast electron transfer rate. The synergistic influence of c-MWCNT, PANI, and CuNPs contributes to the excellent performance for the biosensor.

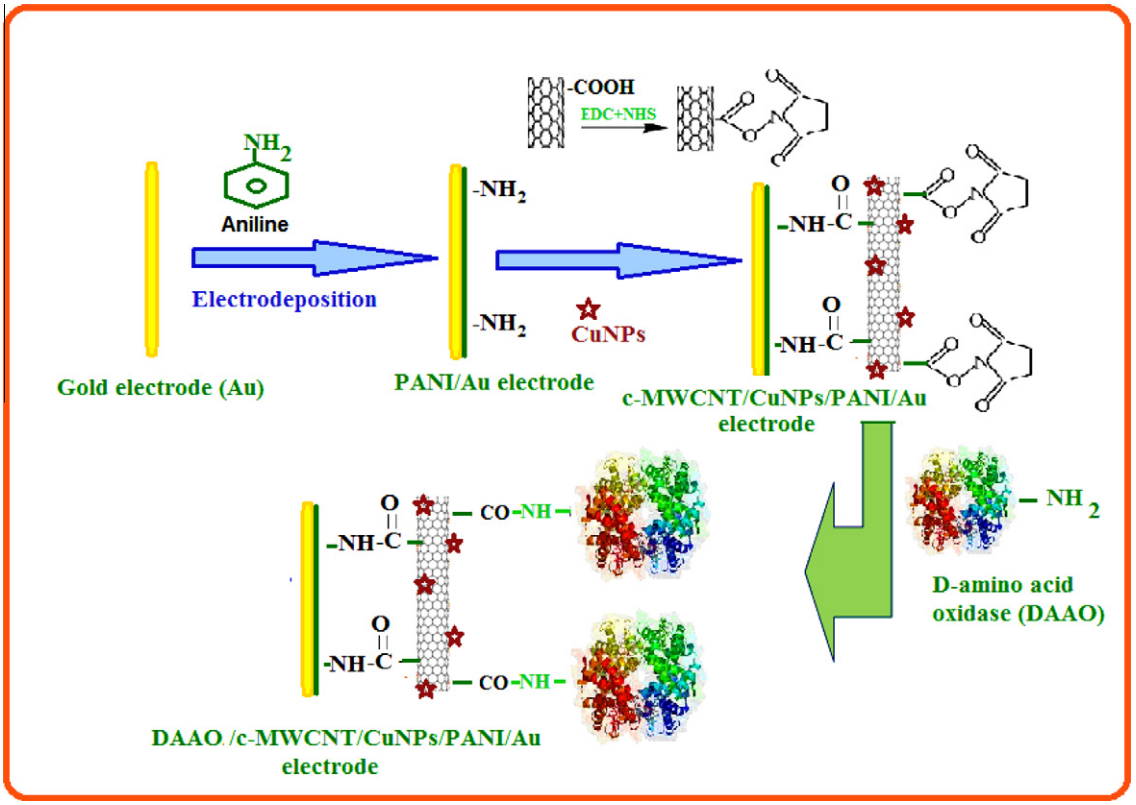

Fig.4. Schematic representation of chemical reactions involved in the fabrication of DAAO/c-MWCNT/CuNPs/PANI/Au electrode.

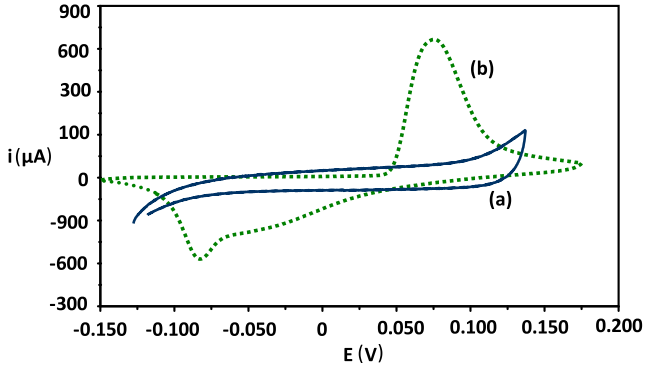

Fig.5. Cyclic voltammograms of the bare Au electrode (curve a) and the electrochemical deposition of c-MWCNT/CuNPs/PANI/Au electrode (curve b) in 0.05 M Tris–HCl buffer (pH 8.0) with 0.1 mM D-Ala. Supporting electrolyte: 0.1 M KCl solution; scan rate: 50 mV s^{-1}.

FTIR spectra

Fig. 6A shows Fourier transform infrared (FTIR) spectra for PANI, c-MWCNT/CuNPs/PANI, and enzyme/c-MWCNT/CuNPs/PANI composites. The spectrum for PANI (Fig. 6A, curve i) exhibited a clear presence of benzoid at 1491.03 cm^{-1} and a quinoid ring vibration at 1548.24 cm^{-1}, indicating the oxidation state of emaraldine salt of PANI. The strong band around 1139.61 cm^{-1} can be attributed to B – N^+ = Q (characteristic peak of PANI conductivity) and a measure of the degree of the delocalization of electrons [32]. The very weak and broad band around 3435 cm^{-1} was assigned to the N–H stretching mode of PANI. In the FTIR spectra of c-MWCNT and CuNPs is a very broad peak at 3399.3 cm^{-1} that corresponds to the –OH group present on c-MWCNTs. When PANI and c-MWCNT composite was formed, no new absorption peak results, but peak shapes change to some extent due to interaction between c-MWCNTs and PANI and CuNPs (Fig. 6A, curve ii). The interaction between the c-MWCNTs and PANI due to charge transfer may result in an increase in the N–H stretching intensity. There was a shift in peak from 3435 to 3419 cm^{-1} and from 1491.03 to 1593.19 cm^{-1}. The enzymes binding on c-MWCNT/CuNPs/PANI/Au electrode were indicated by the appearance of additional absorption bands at 1647.5 and 1589.10 cm^{-1} (Fig. 6A, curve iii), which were assigned to carbonyl stretch (amide I band) and –N–H bonding (amide II band), respectively. In addition, a change in peak position was observed (1636 to 1647.5 cm^{-1} and 1570 to 1540 cm^{-1}), indicating that the DAAO was immobilized onto c-MWCNT/CuNPs/PANI composite film. The successful covalent immobilization of enzyme onto c-MWCNT/CuNPs/PANI composite film was indicated by the appearance of the infrared absorption of the amide I and amide II [33].

Electrochemical impedance measurements

The Nyquist plot (Fig. 6B) displays electrochemical impedance spectroscopy (EIS) studies of PANI/Au (curve a), c-MWCNT/CuNPs/PANI/Au (curve b), and DAAO/c-MWCNT/CuNPs/PANI/Au (curve c) in 0.05 M Tris–HCl buffer (pH 8.0) containing 5 mM $K_3Fe(CN)_6$/$K_4Fe(CN)_6$ (1:1) as a redox probe. The R_{CT} values for the PANI/Au, c-MWCNT/CuNPs/PANI/Au, and DAAO/c-MWCNT/CuNPs/PANI/Au electrodes were obtained as 475, 315, and 390 Ω, respectively. The R_{CT} of c-MWCNT/CuNPs/PANI/Au electrode (curve b) was lower than that of PANI/Au electrode (curve a), revealing its decreased resistance and high electron transfer efficiency. This means that the c-MWCNTs and CuNPs inside the PANI matrix may lead to a faster electron transport in the bulk film and charge transfer in the parallel PANI film interface and c-MWCNT interface compared with that in the originally pure PANI interface. This suggests that the c-MWCNTs and CuNPs have an obvious improvement effect that makes the

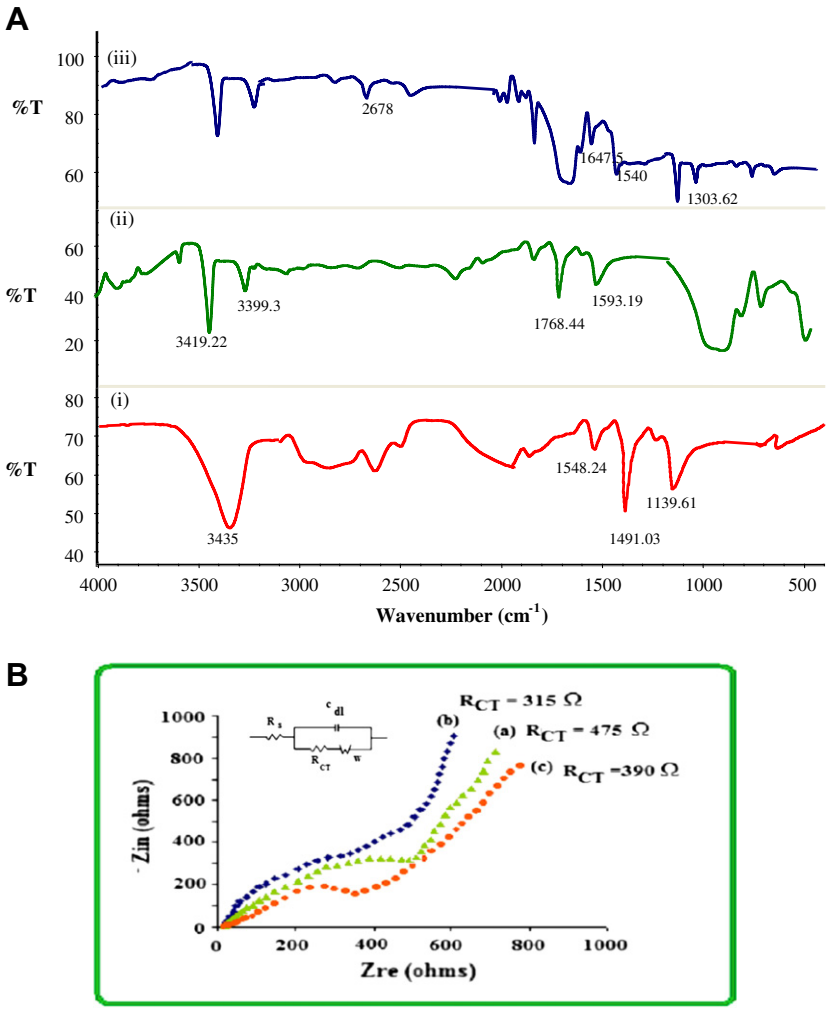

Fig.6. (A) FTIR spectra of PANI/Au electrode (curve i), c-MWCNT/Au electrode (curve ii), and DAAO/c-MWCNT/CuNPs/PANI/Au electrode (curve iii). (B) Impedance spectra of bare Au electrode (curve a), c-MWCNT/CuNPs/PANI/Au electrode (curve b), and DAAO/c-MWCNT/CuNPs/PANI/Au electrode (curve c) in 0.05 M Tris–HCl buffer (pH 8.0) containing $[K_3Fe(CN)_6]^{3-}/[K_3Fe(CN)_6]^{4-}$ (0.05 M).

composite have more active sites for Faradaic reactions. This may lead to enhanced conductivity of modified Au electrode due to lower resistance and, thus, facilitates the charge transfer of the composite. However, the R_{CT} of DAAO/c-MWCNT/CuNPs/PANI/Au enzyme electrode (curve c) increased compared with that of c-MWCNT/CuNPs/PANI/Au electrode. This increase in R_{CT} can be attributed to the fact that most biological molecules, including enzymes, are poor electrical conductors at low frequencies and cause hindrance to electron transfer. These results also indicate the binding of enzymes onto c-MWCNT/CuNPs/PANI composite.

Optimization of D-amino acid biosensor

The biosensor showed the optimal response at pH 8.0, which is similar to that of earlier biosensors based on activated controlled pore glass (pH 8.0) [19] and Amberzyme oxirane support (pH 8.0) [22] but higher than that of biosensors based on silica gel (pH 5.3) [17], eggshell membrane (pH 7.0) [20], and PB and Nafion layer (pH 7.4) [21] (Table 1). The biosensor response increases as the incubation temperature increases up to 30 °C, after which it declines rapidly because of the denaturation of enzyme (DAAO). The optimal temperature of the current biosensor was comparable to those of earlier DAA biosensors (Table 1). Hence, the subsequent experiments were performed at 30 °C. There was a hyperbolic relationship between biosensor response and D-Ala concentration in the range of 0.001 to 1.0 mM, and the response was constant after 0.65 mM. The linear plot reveals that enzyme electrode can work well in DAA solution with a sensitivity of 54.85 μA/mM/cm^2.

Evaluation of biosensor

Linearity

There was a linear relationship between the current (in μA) and the D-Ala concentration in the range of 0.001 to 0.650 mM (Table 1).

Detection limit

The detection limit of the current sensor was 0.2 μM (signal/noise = 3), with the limit of quantification (LOQ = 10 (standard deviation of response of biosensor/slope of calibration curve) being 0.03 μM, which is lower than those of earlier biosensors (Table 1).

Analytical recovery

Analytical recoveries of exogenously added 0.5 and 1.0 mM DAAs in fruit juice by the current method were 98% and 97%, respectively, showing the high reliability of the method (Table 2).

Precision

To check the reproducibility and reliability of the current DAA biosensor, the DAA contents of the fruit juice in one run

Table 1
Comparison of analytical properties of current DAAO/c-MWCNT/CuNPs/PANI/Au electrode with earlier DAA biosensors.

Property	Ref. [17]	Ref. [18]	Ref. [20]	Ref. [21]	Ref. [22]	Ref. [23]	Ref. [24]	Ref. [34]	Current work
Source of DAAO	Porcine kidney	Porcine kidney	Porcine kidney	Porcine kidney	Porcine kidney	*Rodotorrula gracillis*	Goat kidney	Goat kidney	Porcine kidney
Support of immobilization	Silica gel	Graphite–Teflon electrode	Activated controlled pore glass	Eggshell membrane	PB and Nafion layer	Amberzyme oxirane support	Nickel hexacyanoferrate polypyrrole hybrid film	Poly(indole-5-carboxylic acid)/zinc sulfide nanoparticles hybrid film	c-MWCNT/CuNPs/PANI/Au
Method for immobilization	Cross-linking	NR	Adsorption	Cross-linking	Adsorption	Cross-linking	Adsorption	Covalent	Covalent
Type of transducer	Chemiluminescence	Amperometric	FIA system	DO metric	Amperometric	Amperometric	Amperometric	Amperometric	Amperometric
Working optimal pH	5.3	9.0	8.0	7.0	7.4	8.0	7.0	7.5	8.0
Optimal temperature (°C)	40	30	30	44	NR	30	35	35	30
Response time	NR	NR	NR	1 min	NR	10–15 min	1 s	3 s	2 s
Linearity	1.11×10^{-6} to 2.1×10^{-4} M	$5.0–50 \times 10^{-4}$ M	0.1–1.0 mM	0.05–1.5 mM	50–200 μM	0.25–5.0 mM	20–500 μM.	0.001–20 mM	0.2 μM to 0.650 mM
Detection limit	0.45 μM	28 μM	50 μM	30 μM	1 μM	50 μM	1.5 μM	1 μM	0.2 μM
Storage stability	NR	NR	1 week	2 months	10 days	2 weeks	2 months	>2 months	4 months
K_m	0.5 mM	0.25 mM	NR	0.3 mM	0.41 mM	0.9 mM	NR	0.8 mM	0.35 mM
Application	Serum sample	Food sample	Fish sauce	Serum sample	Fruit juices and milk sample	All DAAs	Fruit juices, serum, and urine	Fruit and vegetable juices	Fruit juices

NR=Not reported, FIA=Flow Injection Analysis, DO=Dissolved Oxygen.

Table 2
Analytical recovery of added D-Ala in fruit juice, as measured by DAA biosensor based on DAAO bound to c-MWCNT/CuNPs/PANI/Au electrode.

DAA added	DAA (mM)	(%) Recovery
–	0.95	100
0.5	1.44	98
1.0	1.92	97

Table 3
Within- and between-assay coefficients of variation for determination of DAA in fruit juices, as measured by DAA biosensor based on DAAO bound to c-MWCNT/CuNPs/PANI/Au electrode.

n	Mean (mM)	CV (%)	Relative standard deviation (%)
Within assay (6)			
1.22	1.25	3.4	3.41
1.31			
1.26			
1.28			
1.25			
1.19			
Between assay (6)			
1.38	1.305	4.5	4.57
1.32			
1.35			
1.29			
1.28			
1.21			

(within-batch) and after storage at −20 °C for 1 week (between-batch) were determined. The results showed that the DAA values of these determinations agreed with each other, and the within-batch and between-batch coefficients of variation (CVs) were 3.4% and 4.5%, respectively (Table 3), showing the good reproducibility and reliability of the method.

Application of DAA biosensor

To study the accuracy of the current method, DAA levels in 25 fruit juices as determined by the current method (y) were compared with those obtained by the standard chemical spectrophotometric method (x). When the commercially available fruit juice DAA values obtained by the current method were compared with those obtained by the chemical spectrophotometric method, there was a good correlation ($r = 0.9768$) with the following regression equation: $y = 0.9553x + 0.0268$ (Fig. 7) with 3% bias [(average of test measurement−average of reference method) × 100]. These results show high accuracy of the current method.

Interference study

The interference study of the current DAA biosensor was carried out by comparing the amperometric response before and after adding some interferents such as uric acid, ascorbic acid, glycine, glucose, and uric acid along with 100 μM D-Ala in 0.05 M Tris–HCl (pH 8.0) at their physiological concentrations. The results showed negligible interference of these substances.

Stability and reusability of enzyme electrode

The stability of enzyme electrode was investigated by measuring current response of the biosensor every week under its storage at 4 °C. The enzyme electrode maintained 70% of its initial activity even after 140 days of regular 150 uses (Fig. 8), indicating the better stability of the current enzyme electrode than earlier enzyme electrodes (stability 7–60 days) [19–22] (Table 1). This can be

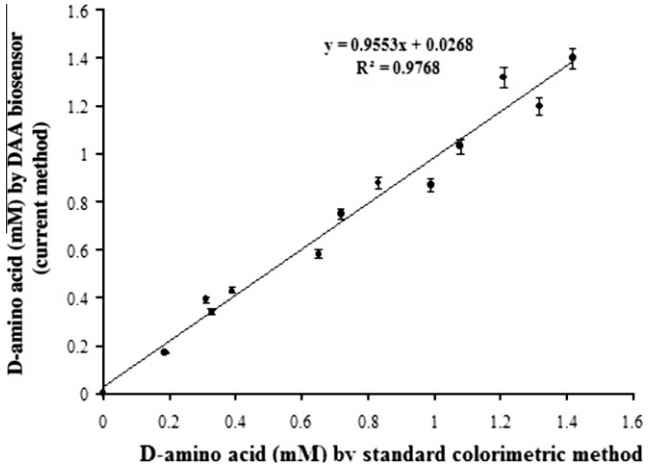

Fig.7. Correlation between fruit juice values measured by the standard colorimetric method (*x* axis) and those measured by the current method (*y* axis) employing the DAA biosensor based on c-MWCNT/CuNPs/PANI/Au composite film.

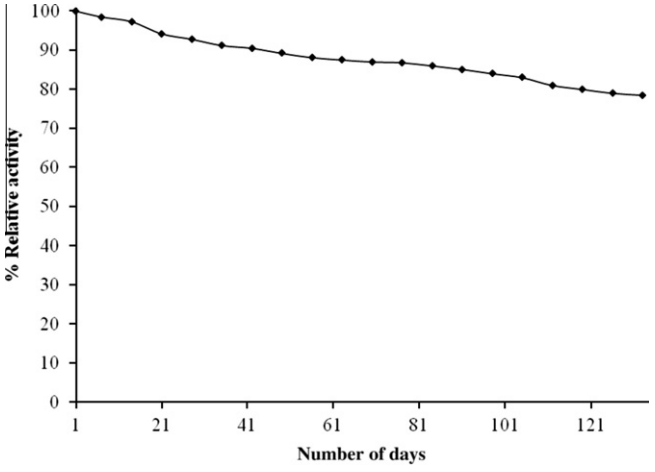

Fig.8. Effect of storage at 4 °C on the response of DAAO/c-MWCNT/CuNPs/PANI/Au electrodes.

attributed to the covalent immobilization of DAAO onto the c-MWCNT/CuNPs/PANI/Au electrode.

Summary and conclusion

An improved amperometric DAA biosensor was constructed by covalent immobilization of DAAO onto c-MWCNT/CuNPs/PANI hybrid film modified Au electrode. The biosensor was highly specific, more rapid (2 s response time), and sensitive (54.85 μA/mM/cm^2), with a detection limit of 0.2 μM and a broader working range (0.001–0.650 mM), good reproducibility, and high storage stability (140 days). It is concluded that the use of this hybrid film improves the analytical performance of the DAA biosensor and could also be employed for the improvement of other biosensors.

Acknowledgments

Suman Lata and Bhawna Batra are thankful to the Council of Scientific and Industrial Research (CSIR) New Delhi, India) for the award of a Senior Research Fellowship and a Junior Research Fellowship, respectively, during this study.

References

[1] W. Leuchtenberger, K. Huthmacher, K. Drauz, Biotechnological production of amino acids and derivatives: current status and prospects, Appl. Microbiol. Biotechnol. 69 (2005) 1–8.
[2] M. Friedman, R. Liardon, Racemization kinetics of amino acid residues in alkali-treated soybean proteins, J. Agric. Food Chem. 33 (1985) 666–672.
[3] M. Fuse, F. Hayase, H. Kato, Digestibility of proteins and racemization of amino acid residues in roasted foods, J. Jpn. Soc. Nutr. Food Sci. 37 (1984) 348–354.
[4] F. Hayase, H. Kato, M. Fujimaki, Racemization of amino acid residues in protein during roasting, Agric. Biol. Chem. 37 (1973) 191–192.
[5] G. Palla, R. Marchelli, A. Dossena, G. Casnati, Occurrence of D-amino acids in food: detection by capillary gas chromatography and by reversed-phase high-performance liquid chromatography with L-phenylalanine amides as chiral selectors, J. Chromatogr. 475 (1989) 45–53.
[6] D.A. Reaveley, R.E. Burge, Walls and membranes in bacteria, Adv. Microb. Physiol. 7 (1972) 1–81.
[7] H. Bruckner, D. Becker, M. Lupke, Chirality of amino acids of microorganism used in food technology, Chirality 5 (1993) 385–392.
[8] J.S. Kim, Y.S. Lee, Enolization and racemization reactions of glucose and fructose on heating with amino-acid enantiomers and the formation of melanoidins as a result of the Maillard reaction, Amino Acids 36 (2009) 465–474.
[9] M. Calabrese, B. Stancher, P. Riccobon, High performance liquid chromatography determination of proline isomers in Italian wines, J. Sci. Food Agric. 69 (1995) 361–366.
[10] P. Sarkar, I.E. Tothill, S.J. Setford, A.P.F. Turner, Screen printed amperometric biosensors for the rapid measurement of L- and D-amino acids, Analyst 124 (1999) 865–870.
[11] K. Hamase, A. Morikawa, T. Ohgusu, W. Lindner, K. Zaitsu, Comprehensive analysis of branched aliphatic D-amino acids in mammals using an integrated multi-loop two-dimensional column-switching high-performance liquid chromatographic system combining reversed-phase and enantioselective columns, J. Chromatogr. A 114 (2007) 3105–3111.
[12] M. Friedman, Origin, microbiology, nutrition, and pharmacology of D-amino acids, Chem. Biodivers. 71 (2010) 491430.
[13] Q. Chi, S. Dong, Amperometric biosensors based on the immobilization of oxidases in a Prussian Blue film by electrochemical codeposition, Anal. Chim. Acta 310 (1995) 429–436.
[14] S. Sacchi, E. Rosini, L. Caldinelli, L. Pollegioni, Biosensors for D-amino acid detection, Methods Mol. Biol. 794 (2012) 313–324.
[15] M. Loughran, H. Ren, E. Watanabe, Some voltammetric conditions for the determination of D- and L-amino acids, Tokyo Suisandai Kempo 85 (1998) 43–52.
[16] M. Váradi, N. Adanyi, E.E. Szabo, N. Trummer, Determination of the ratio of D- and L-amino acids in brewing by an immobilised amino acid oxidase enzyme reactor coupled to amperometric detection, Biosens. Bioelectron. 14 (1999) 335–340.
[17] B.X. Li, Z. Zhang, Chemiluminescence flow biosensor for determination of total D-amino acid in serum with immobilized reagents, Sens. Actuators B 69 (2000) 70–74.
[18] R. Dominguez, B. Serra, J. Revieo, J.M. Pingarron, Chiral analysis of amino acids using electrochemical composite bienzyme biosensors, Anal. Biochem. 298 (2001) 275–282.
[19] Y. Inaba, K. Mizukami, N. Hamada-Sato, T. Kobayashi, C. Imada, E. Watanaba, Development of a D-alanine sensor for the monitoring of a fermentation using the improved selectivity by the combination of D-amino acid oxidase and pyruvate oxidase, Biosens. Bioelectron. 19 (2003) 423–431.
[20] G. Zhang, D. Liu, S. Shuang, M.F. Martin, A homocysteine biosensor with eggshell membrane as an enzyme immobilization platform, Sens. Actuators B 114 (2006) 936–942.
[21] M. Wcislo, D. Compagnone, M. Trojanowic, Enantioselective screen-printed amperometric biosensor for the determination of D-amino acids, Bioelectrochemistry 71 (2007) 91–98.
[22] E. Rosini, G. Molla, C. Rossetti, M.S. Pilone, L. Pollegioni, S. Sacchi, A biosensor for all D-amino acids using evolved D-amino acid oxidase, J. Biotechnol. 135 (2008) 377–384.
[23] Z.M. Zain, R.D. O'Neill, J.P. Lowry, M. Pierce, K.W. Tricklebank, A. Dewa, S.A. Ghani, Development of an implantable D-serine biosensor for in vivo monitoring using mammalian D-amino acid oxidase on a poly(*o*-phenylenediamine) and Nafion-modified platinum–iridium disk electrode, Biosens. Bioelectron. 25 (2010) 1454–1459.
[24] S. Lata, C.S. Pundir, Fabrication of an amperometric D-amino acid biosensor based on nickel hexacyanoferrate polypyrrole hybrid film deposited on glassy carbon electrode, Bioprocess Biosyst. Eng. 36 (2013) 81–89.
[25] S. Lata, B. Batra, N. Karwasra, C.S. Pundir, An amperometric H_2O_2 biosensor based on cytochrome *c* immobilized onto nickel oxide nanoparticles/carboxylated multiwalled carbon nanotubes/polyaniline modified gold electrode, Process Biochem. 47 (2012) 992–998.
[26] D. Tasis, N. Tagmatarchis, A. Bianco, M. Prato, Chemistry of carbon nanotubes, Chem. Rev. 106 (2006) 1105–1136.
[27] D. Wei, A. Ivaska, Electrochemical biosensors based on polyaniline, Chem. Anal. (Warsaw) (2006) 839 (review).
[28] R. Sainz, M. Ana, M. Benito, M. Teresa, F.G. Juan, S. Javier, M.B. Arturo, C. Benoit, C. Olivier, K.M. Wolfgang, Soluble self-aligned carbon nanotube/polyaniline composites, Adv. Mater. 17 (2005) 278–281.

[29] E.B. Arias, J.C. Cancho, D.L. Gonzalez, J.M. Serrano, Use of an enzyme assay in student classes, Biochem. Educ. 20 (1992) 234–235.
[30] Q. Zhang, Z.M. Yang, B.J. Ding, X.Z. Lan, Y.J. Guo, Preparation of copper nanoparticles by chemical reduction method, Trans. Nonferrous Met. Soc. China 20 (2010) 240–244.
[31] H. Szu, D.H.C. Wu, Synthesis of high-concentration Cu nanoparticles in aqueous CTAB solutions, J. Colloid Interface Sci. 273 (2004) 165–169.
[32] S. Quillard, G. Louarn, S. Lefrant, A.G. Macdiarmad, Vibrational analysis of polyaniline: a comparative study of leucoemeraldine, emeraldine, and pernigraniline bases, Phys. Rev. B 50 (1994) 12496–12508.
[33] Z. Matharu, G. Sumana, S.K. Arya, B.P. Singh, V. Gupta, Polyaniline Langmuir–Blodgett film based cholesterol biosensor, Langmuir 23 (2007) 13188–13192.
[34] S. Lata, B. Batra, C.S. Pundir, Construction of D-amino acid biosensor based on D-amino acid oxidase immobilized onto poly(indole-5-carboxylic acid)/zinc sulfide nanoparticles hybrid film, Process Biochem. 47 (2012) 2131–2138.